The Mechanical, Thermal and Morphological Properties of Graphene Nanoplatelets Filled Poly(lactic acid)/Epoxidized Palm Oil Blends

Buong Woei Chieng[1,*], Nor Azowa Ibrahim [1], Wan Md Zin Wan Yunus [2] and Mohd Zobir Hussein.[3]

[1]Department of Chemistry, Faculty of Science, Universiti Putra Malaysia, 43400 UPM Serdang, Selangor, Malaysia
[2]Department of Defence Science , Faculty of Defence Science and Technology, National Defence University of Malaysia, 57000 Kuala Lumpur, Malaysia
[3]Material Synthesis and Characterization Laboratory, Institute of Advance Technology, Universiti Putra Malaysia, 43400 UPM Serdang, Selangor, Malaysia
* chieng891@gmail.com / chieng@upm.edu.my

ABSTRACT

Poly(lactic acid) (PLA)-based nanocomposites filled with graphene nanoplatelets (xGnP) that contains epoxidized palm oil (EPO) as plasticizer were prepared by melt blending method. PLA was first plasticized by EPO to improve its flexibility and thereby overcome its problem of brittleness. Then, xGnP was incoporated into plasticized PLA to enhance its mechanical properties. Plasticized and nanofilled PLA nanocomposites (PLA/EPO/xGnP) showed improvement in the elongation at break by 3322% and 61% compared to pristine PLA and PLA/EPO, respectively. The use of EPO and xGnP increases the mobility of the polymeric chains, thereby improving the flexibility and plastic deformation of PLA. The nanocomposites also resulted in an increase of up to 26.5% in the tensile strength compared with PLA/EPO blend. XRD pattern showed the presence of peak around 26.5° in PLA/EPO/xGnP nanocomposites which corresponds to characteristic peak of graphene nanoplatelets. Plasticized PLA reinforced with xGnP showed that increasing the xGnP content triggers a substantial increase in thermal stability. Crystallinity of the nanocomposites as well as cold crystallization and melting temperature did not show any significant changes upon addition of xGnP. However, there was a significant decrease of glass transition temperature up to 0.3wt% of xGnP incorporation. The TEM micrograph of PLA/EPO/xGnP shows that the xGnP was uniformly dispersed in the PLA matrix and no obvious aggregation was observed.

***Keywords**: graphene nanoplatelets, plasticizers, poly(lactic acid)*

ISSN 1675-7009

INTRODUCTION

Poly(lactic acid) (PLA) is an attractive candidate for replacing petrochemical polymer because it is biodegradable and produced from renewable resources. Suppliers claim that by using the right additives, PLA performances can be made comparable to those of polystyrene (PS), poly(ethylene terephthalate) (PET), polyethylene (PE), poly(vinyl chloride) (PVC), etc. and it can replace these or other non-biodegradable resins in many applications.

PLA is characterized by excellent optical properties and high tensile strength but unfortunately, it is rigid and brittle. There is a general interest to formulate new grades of PLA with improved flexibility, ductility, and higher impact properties, while the tensile strength performances are maintained at the optimal level due to the current limitation required by a few applications such as packaging. A large number of investigations have been made to improve PLA properties via plasticization but due to several variables being involved such as nature of PLA matrix, type, and optimal percentage of plasticizer, thermal stability at the processing temperature, etc., unfortunate poor mechanical properties and/or the relationship between the thermo-mechanical properties and molecular parameters have not been considered enough. Plasticizers such as, citrate esters [1-3], citrate oligomers [4], triacetine [2, 5], glycerol [6], oligomeric malonate esteramides [7, 8], glucosemonoesters [9], and oligomeric lactic acid (OLA) [6], epoxidized palm oils [10, 11], poly(1,3-butylene adipate) [12], poly(ethylene glycol) [3, 6, 9, 13, 14], poly(propylene glycol) [15, 16], were used to improve the flexibility and impact resistance of PLA. The resulting plasticized PLA materials gained in deformation and resilience.

Epoxidized Palm Oil (EPO) is one of the vegetable oils with high potential as plasticizer for bioplastics. Palm oil is a suitable vegetable oil based on its low cost, low toxicity, and its availability as a renewable agricultural resource. It is derived from oil palm trees which are one of the most economical perennial oil producing crops in Malaysia. It belongs to the species *Elaeis guineensis* under the family *Palmacea* and originated in the tropical forests of West Africa. EPO are used extensively as plasticizers, stabilizers, and additives for many polymers [17].

Concerning the mechanical properties of PLA, it can be improved by addition of nano-sized filler. Various nano-reinforcement filler, such as layered silicate clay [18], carbon nanotubes [19] and layered double-hydroxide [20] are being developed and extensively studied. However, the discovery of new nano-material graphene by Andre Geim in year 2004 [21], gained interest among researchers worldwide. Graphene, which is fabricated from natural graphite can be used as a potential alternative nano-reinforcement to both clay and carbon nanotubes. Graphene Nanoplatelets (xGnP) are recently developed nanomaterials that are formed by stacks of short disk-like layers of graphite. It combines layered structure of clays with superior mechanical and thermal properties of carbon nanotubes, which can provide excellent functional properties enhancements [22]. Graphite is the stiffest material found in nature having a modulus several times higher compared to clay, accompanied with its excellent strength, electrical and thermal conductivity, hence it is claimed to have similar properties as carbon-based nanomaterials [23]. Furthermore, xGnP is much cheaper compared to either single-walled or multi-walled carbon nanotubes.

In this study, Poly(lactic acid) (PLA)-based nanocomposites filled with graphene nanoplatelets (xGnP) and containing epoxidized palm oil (EPO) as plasticizer were prepared by

ISSN 1675-7009

melt blending method. The compositions were fully characterized by mechanical, thermal and morphological properties.

MATERIALS AND METHODS

Poly(lactic acid) resin, commercial grade 4042D, was supplied by NatureWorks® LCC, Minnesota USA. Epoxidized palm oil (pH value of about 5 – 6) was supplied by Malaysian Palm Oil Board (MPOB, Malaysia). The acid value and viscosity at 25 ^{o}C of the EPO was 0.09 mg KOH g^{-1} and 70.7 cP, respectively. Graphene nanoplatelets, trade name xGnP®, was supplied by XG sciences Inc, Michigan. Each particle consists of several sheet of graphene with an average thickness of approximately 6–8 nanometers, average diameter of 15 microns.

Preparation of PLA/EPO/xGnP nanocomposites

The PLA/EPO/xGnP nanocomposites were melted and blended by Brabender internal mixer with 25 rpm of the rotor speed, at 160 ^{o}C for 10 min. EPO was used as plasticizer to PLA. The weight ratio of PLA to EPO studied is fixed at 95/5. The EPO plasticized PLA was labeled as p-PLA throughout this study. The xGnP content was varied between 0.1 wt% to 1.0 wt%. The composites obtained were then molded into sheets of 1 mm in thickness by hot pressing at 160 ^{o}C for 10 min at the pressure of 110 kg/cm^2, followed by cooling to room temperature. The sheets were used for further characterization.

Characterizations

Tensile properties test were carried out by using Instron 4302 series IX (Buckinghamshire, UK) attached with 1.0 kN load cell at room temperature with constant crosshead speed of 10 mm/min. The samples were cut into dumbbell shape according to ASTM D638 (type V) standard. X-ray diffraction (XRD) measurement was carried out using Shimadzu XRD 6000 X-ray diffractometer (Tokyo, Japan) with CuK_{α} radiation (λ=1.542 Å) operated at 30 kV and 30 mA. Data were recorded in 2θ range of 2 ^{o} – 10 ^{o} at the scan rate of 2 ^{o}/min. Differential Scanning calorimetry (DSC) analysis was performed using a Perkin Elmer DSC 7 (Waltham, MA, USA) to study the nonisothermal crystallization kinetics. Thermogravimetric analysis (TGA) was carried out using a Perkin Elmer Pyris 7 TGA (Waltham, MA, USA) analyzer with scan range from 35 ^{o} to 800 ^{o} at a constant heating rate of 10 ^{o}C/min and continuous nitrogen flow. The morphological observations of the prepared nanocomposite was made by Scanning Electron Microscopy (SEM), JEOL JSM-6400 (Tokyo, Japan) and Transmission Electron Microscope (TEM), Hitachi H7100 (Tokyo, Japan).

ISSN 1675-7009

RESULTS AND DISCUSSION

X-ray diffraction (XRD)

XRD is an effective method to determine the existence of xGnP as individual graphene sheets in the nanocomposites. Figure 1 shows the XRD patterns of as-received xGnP, p-PLA and p-PLA nanocomposite with various xGnP loading. The xGnP exhibits an intense peak at 2θ value of ~26.4°, assigned to the stacking of the single graphene layers at a distance of 0.34 nm [24]. There is no other peak observed for xGnP. Alternatively, the XRD patterns of p-PLA and p-PLA with various xGnP loadings exhibit an initial broad characteristic peak of PLA matrix at 2θ = ~16°. Notice that, there was no xGnP's peak observed for p-PLA/0.1 wt% which may be due to the low amount of ordered layer structure of xGnP. The disappearance of peak may also be due to the exfoliation and random distribution of the platelets within the polymer matrices at low loading of xGnP [25].

A small peak around 26.5° which corresponds to characteristic peak of xGnP start emerges at 0.3 wt% xGnP loading in p-PLA nanocomposites, showing that the graphene layer is unable to disperse or completely separate and some sheets are still present in stacks form. The intensity of this peak increases as the xGnP loading increases. The increased intensity recorded at higher xGnP loading could be attributed to the higher number of graphene layers organized in stacks. Similar result has been previously reported and the peak observed of reduced intensity was associated to a lower number of graphene stacks [26].

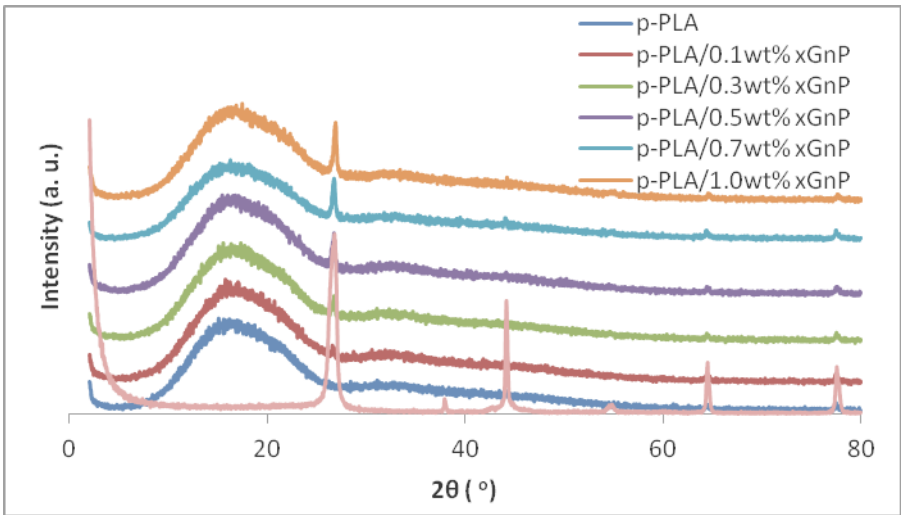

Figure 1: X-ray diffraction patterns of xGnP, p-PLA and p-PLA nanocomposites.

ISSN 1675-7009

Tensile Properties

Tensile properties of the p-PLA/xGnP nanocomposites containing various xGnP contents were examined at room temperature. The effect of xGnP loading on tensile strength of p-PLA composites is depicted in Figure 2(a). The aim of incorporating xGnP into the polymer matrix is to improve its mechanical properties. The homogeneity of composites, orientation of the reinforcements and the strong interfacial interaction between xGnP and the polymer matrix should have a significant effect on the mechanical properties.

Pristine PLA and plasticized PLA (p-PLA) shows tensile strength of 57.9 MPa and 32.5 MPa, respectively. Tensile strength of p-PLA increased as xGnP loading increases and attains the highest value (41.1 MPa) at 0.3 wt% xGnP loading. At 0.1 wt% of xGnP loading, the reinforcement effect is limited due to the density of filler is not high enough to form a percolated network. As illustrated in Figure 3(a), even complete randomization of the xGnP at very low concentration (0.1 wt%) will not result in graphene contact since their spheres of rotation will not intersect. For 0.3 wt% xGnP loading, the xGnP dispersion and distribution started to improve when the xGnP concentration becomes greater. Therefore, the tensile results imply better strength compared to 0.1 wt% xGnP loading. There is xGnP-xGnP and xGnP-matrix interaction as a result of the percolated network formed (Figure 3(b)). Further increase of xGnP loading, decreases the tensile strength. In the concentrated regime of xGnP (>0.5 wt%), reorientation cannot be achieved due to excluded volume interactions between nanoplatelets (Figure 3(c)). When the amount of xGnP reaches a critical content (0.3 wt%) and the distance between two xGnP is so small that they may be apt to stack together easily due to Van der Waals forces [27], thus it decreases in tensile strength.

Figure 2(b) shows the elongation at break of p-PLA/xGnP composites. p-PLA shows elongation at break value of 114.4%. It increases with the addition of xGnP. The highest elongation at break (183.7%) is observed from p-PLA with 0.3 wt% xGnP loading. Further addition of xGnP causes the decrease of elongation at break which made the blend more brittle. The reason for this may be attributed to a large aspect ratio of the rigid filler and the interaction between xGnP and the matrix, which restricts the movement of the polymer chains [27]. The trend of the elongation at break is the inverse of the tensile modulus.

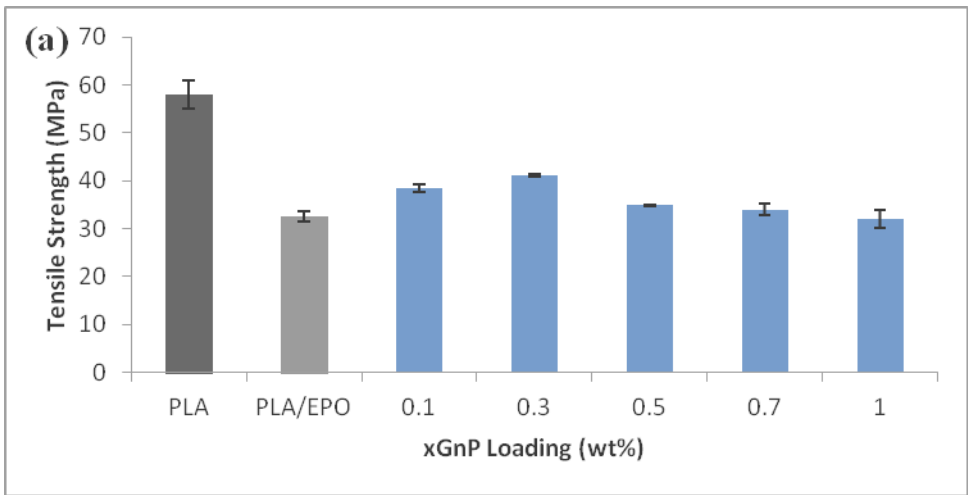

ISSN 1675-7009

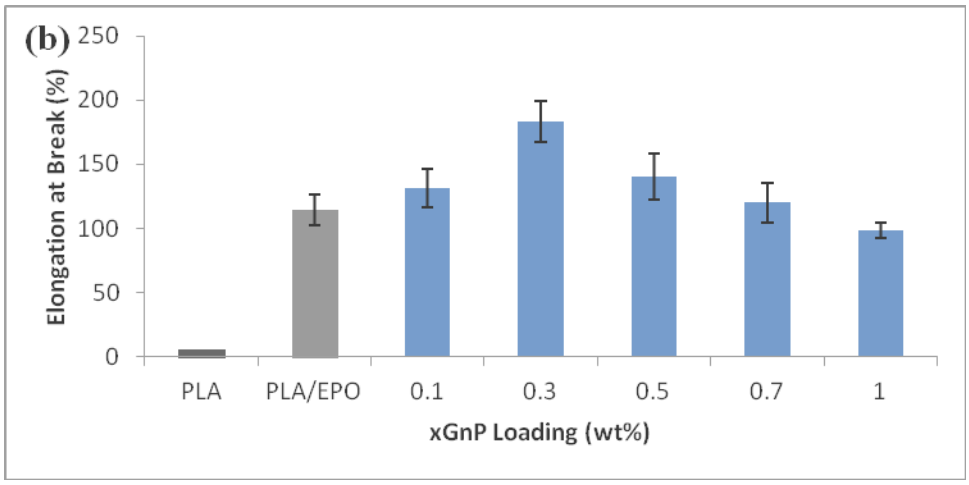

Figure 2: (a) Tensile strength and (b) elongation at break of p-PLA/xGnP nanocomposites

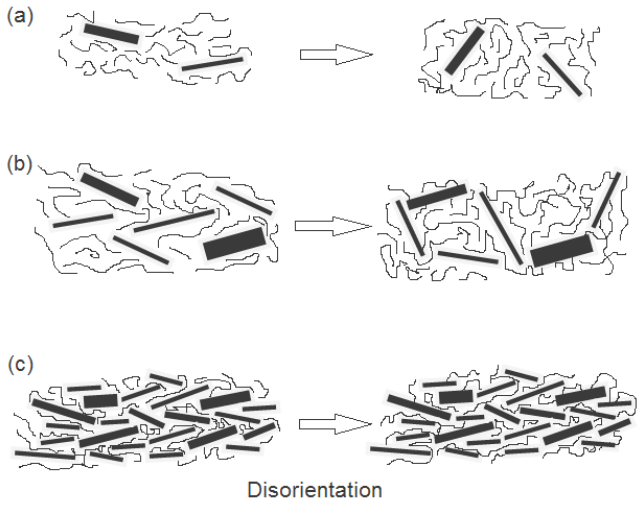

Figure 3. Illustration of disorientation mechanism of xGnP at (**a**) 0.1 wt%; (**b**) 0.3 wt% and (**c**) >0.5 wt%.

From the mechanical tensile test, it can be concluded that there is presence of a critical amount of xGnP loading on the mechanical properties. The critical amount of xGnP loading is 0.3 wt%. At this critical amount, the xGnP is well dispersed in the polymer matrix and brings about significant improvement to the mechanical properties, while further addition of xGnP may result in stacking of the nanoplatelets, lowering the efficiency of the mechanical improvement.

Differential Scanning Calorimetry (DSC)

Differential Scanning Calorimetry (DSC) measures the amount of heat energy absorbed or released when the material is heated or cooled. For polymeric materials, which undergo

ISSN 1675-7009

important property changes near thermal transition, DSC is a very useful technique to study thermal behavior such as glass transition temperature (T_g), cold crystallization temperature (T_{cc}), and melting temperature (T_m). Figure 4 shows the DSC curves of p-PLA and its nanocomposites. Table 1 summarizes the T_g, T_{cc} and T_m of p-PLA and its nanocomposites as well as percentage of crystallinity. The nanocomposites showed cold crystallization above T_g, followed by crystalline melting at ~ 150 ^oC. The T_g, T_{cc} and T_m of p-PLA is 62.62 ^oC, 114.16 ^oC, and 148.12 ^oC, respectively.

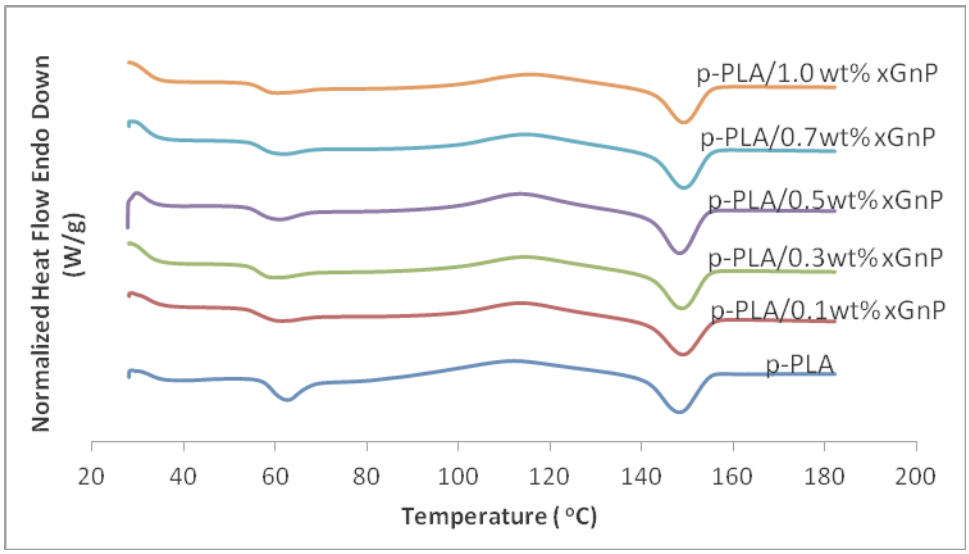

Figure 4: DSC thermograms of p-PLA and p-PLA nanocomposites.

Table 1: Characteristic temperatures and percentage of crystallinity of p-PLA and p-PLA nanocomposites.

	T_g (^oC)	T_{cc} (^oC)	T_m (^oC)	X_c (%)
p-PLA	62.62	114.16	148.12	43.27
p-PLA /0.1wt% xGnP	61.40	113.44	149.00	45.77
p-PLA/0.3wt% xGnP	58.40	114.27	148.67	42.85
p-PLA/0.5wt% xGnP	59.73	113.44	148.16	42.02
p-PLA/0.7wt% xGnP	60.73	114.26	149.17	45.66
p-PLA/1.0wt% xGnP	61.42	115.46	149.03	43.05

The addition of nanofiller in semi-crystalline polymers was found, in general, not to affect considerably the crystallinity of the resulting nanocomposite materials, even though there may be some changes in particular nanocomposite systems [28]. Since PLA is a semicrystalline polymer, its mechanical properties should strongly depend on its crystallinity. Therefore, to confirm the influence of incorporating xGnP into p-PLA on the mechanical enhancement of the composites, DSC is employed to measure the crystallinity difference between p-PLA and p-PLA/xGnP nanocomposites. The crystallinity (X_c) in samples were calculated as follows:

ISSN 1675-7009

$$X_c\,(\%) = \frac{\Delta H_m - \Delta H_{cc} / \Phi_{PLA}}{\Delta H_m^o} \times 100\%$$

where ΔH_m is the measured heat of fusion, ΔH_{cc} is the heat of cold crystallization, Φ_{PLA} is the PLA content in the composites and ΔH_m^o is melting enthalpy of the 100 % PLA (93.6 J/g). As shown in Table 1, the crystallinity of p-PLA nanocomposites showed insignificant changes after adding the xGnP, which corresponds well with the XRD results. The changes of PLA crystallinity is at minimum level that it cannot induce a significant impact on the mechanical properties of the composites. Therefore, the significant reinforcement of the strength and modulus for p-PLA nanocomposites can be mostly attributed to the homogeneous dispersion of xGnP in the polymer matrix and strong interactions between both components [29].

On the other hand, the T_g was found to be affected by the incorporation of the nanofillers. There were no significant changes of T_{cc} and T_m of p-PLA upon addition of xGnP. However, there was a significant decrease in T_g of p-PLA filled with xGnP up to 0.3 wt%. For example, the T_g of p-PLA/0.3 wt% xGnP decreases from 62.62 ^oC to 58.40 ^oC. This result correlates well with the tensile result which showed the increase of elongation at break of the nanocomposite. In previous study by Silverajah et al. [10], the plasticizer EPO does enhance the molecular motions of PLA chains, manifested by decrease of T_g. Moreover, incorporation of xGnP into EPO plasticized PLA further decreases T_g of their nanocomposites. Thus, addition of both nanofiller and plasticizer allowed obtaining a material with lower glass transition temperature and a melting point similar with respect to pristine PLA. On the other hand, the T_g tend to increase at higher xGnP loading (above 0.3 wt%). This may be due to the inability of plasticizer EPO to interact with PLA as it intercalated into interlayer spacing of xGnP. This brings the decrease of plasticization effect to PLA.

Thermogravimetric Analysis (TGA)

Thermal properties of p-PLA and its nanocomposites were investigated by thermogravimetric analysis (TGA). The integral (TG) and derivative (DTG) thermogravimetric curves provide information about the nature and extent of degradation of the polymeric materials. Generally, the incorporation of xGnP into p-PLA is to enhance thermal stability by acting as a superior insulator and mass transport barrier to the volatile products generated during decomposition. Many researchers also have demonstrated that the incorporation of graphenes could enhance the thermal stability of PLA at extremely low loading contents [30, 31]. The TG and DTG thermograms of p-PLA and p-PLA nanocomposites are given in Figure 5. Table 2 shows T_5, T_{50}, T_{95} and T_{max} of p-PLA and p-PLA nanocomposites. T_5, T_{50} and T_{95} refer to the temperature at which the remained mass of the materials is 5 %, 50 % and 95 %, respectively. On the other hand, T_{max} represent maximum decomposition temperature.

Plasticized PLA reinforced with xGnP showed that increasing the filler content triggers a substantial increase in thermal stability. At low filler content, the amount of xGnP might not be sufficient to promote any significant improvement of the thermal stability. However, increasing the xGnP content increases the thermal stability of the nanocomposites. For example, a significant shift from 326.1 ^oC to 360.9 ^oC and 429.1 ^oC to 394.5 ^oC is observed for the T_{95} and T_{max} of p-PLA/1.0wt% xGnP, respectively. The xGnP acts as a heat barrier, which enhances the

ISSN 1675-7009

overall thermal stability of the polymer nanocomposites, as well as assists in the formation of char after thermal decomposition. The xGnP would shift the decomposition to higher temperature at early stages of thermal decomposition. After that, the xGnP layers could hold accumulated heat that could be used as a heat source to accelerate the decomposition process, in conjunction with the heat flow supplied by the outside heat source. Furthermore, the formation of "tortuous path" with exfoliated xGnP also inhibited the passage of volatile degradation products, hence enhancing the thermal stability of the xGnP containing nanocomposites [14].

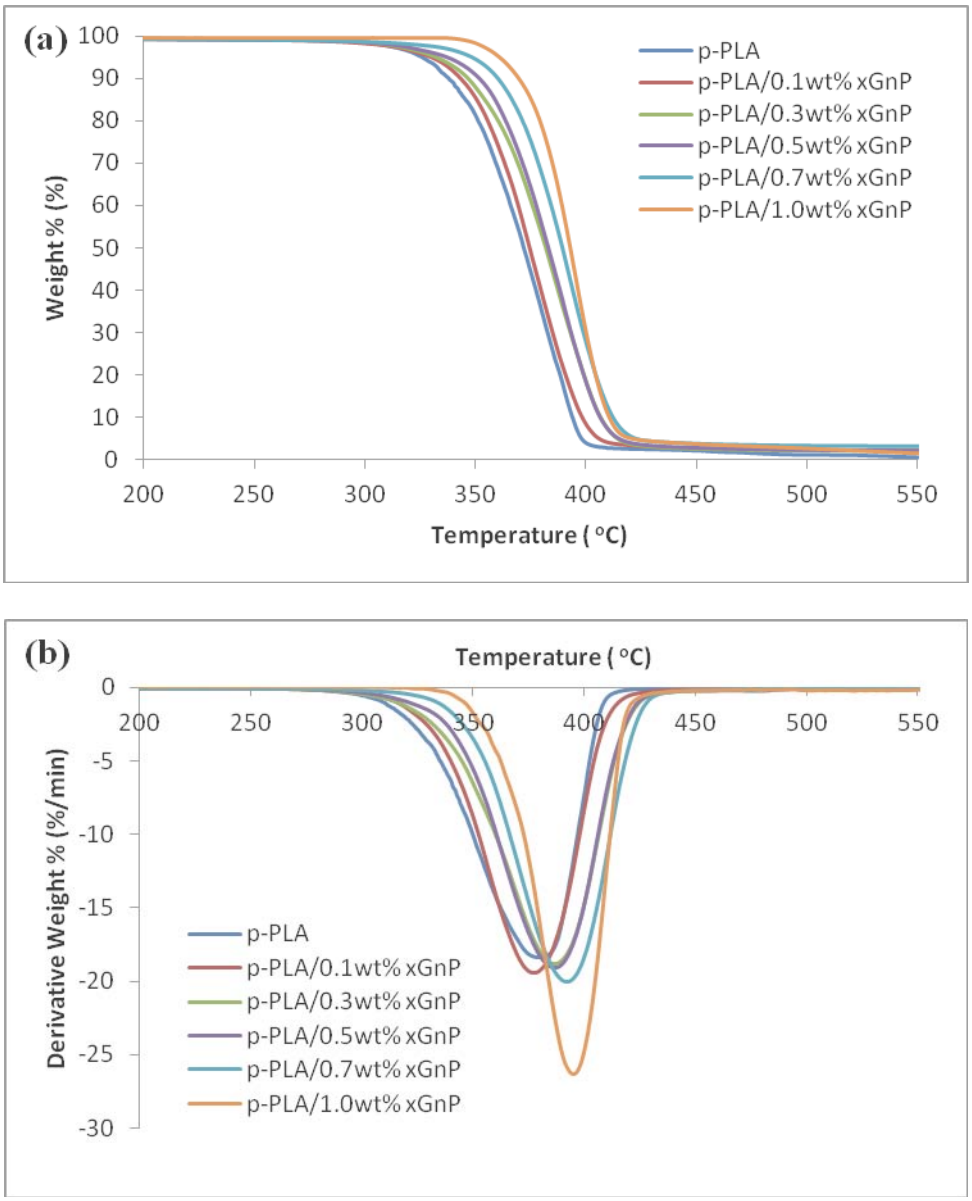

Figure 5: Effect of xGnP on thermal stability of p-PLA and its nanocomposites (a) integral thermogravimetric (TG) and (b) derivative thermogravimetric (DTG) curves.

ISSN 1675-7009

Table 2: Thermal degradation temperature of plasticized PLA and its nanocomposites.

Samples	T_5	T_{50}	T_{95}	T_{max}
p-PLA	397.6	371.7	326.1	429.1
p-PLA/0.1 wt% xGnP	406.0	374.3	330.3	377.5
p-PLA/0.3 wt% xGnP	414.3	381.7	332.6	386.6
p-PLA/0.5 wt% xGnP	414.7	382.9	337.5	386.7
p-PLA/0.7 wt% xGnP	422.0	389.0	349.0	392.2
p-PLA/1.0 wt% xGnP	421.1	392.9	360.9	394.5

Morphology

The fracture surface of the nanocomposites was examined by Scanning Electron Microscope (SEM) and Transmission Electron Microscope (TEM) to study the morphology of the nanocomposite. Figure 6(a) and 6(b) show SEM and TEM micrographs of fracture surface of p-PLA/0.3wt% xGnP, respectively. As shown in Figure 6(a), the dark background represents the PLA polymer matrix while bright areas represent xGnP sheets (as shown by the arrow) distributed in the polymer matrix. The conducting xGnP and the insulating polymer matrix resulted in the contrast between xGnP network and polymer matrix. The p-PLA/0.3 wt% xGnP nanocomposite showed homogenous and good uniformity. Good uniformity of composites indicates good degree of dispersion of the nanofiller and therefore results in better tensile strength. p-PLA/0.3 wt% xGnP also exhibit a strong stretching effect conforming to the high elongation at break during tensile testing. This agrees with the elongation at break result which gives the highest values (183.7%). The TEM micrograph of PLA/EPO/xGnP shows that the xGnP was uniformly dispersed in the PLA matrix and no obvious aggregation was observed.

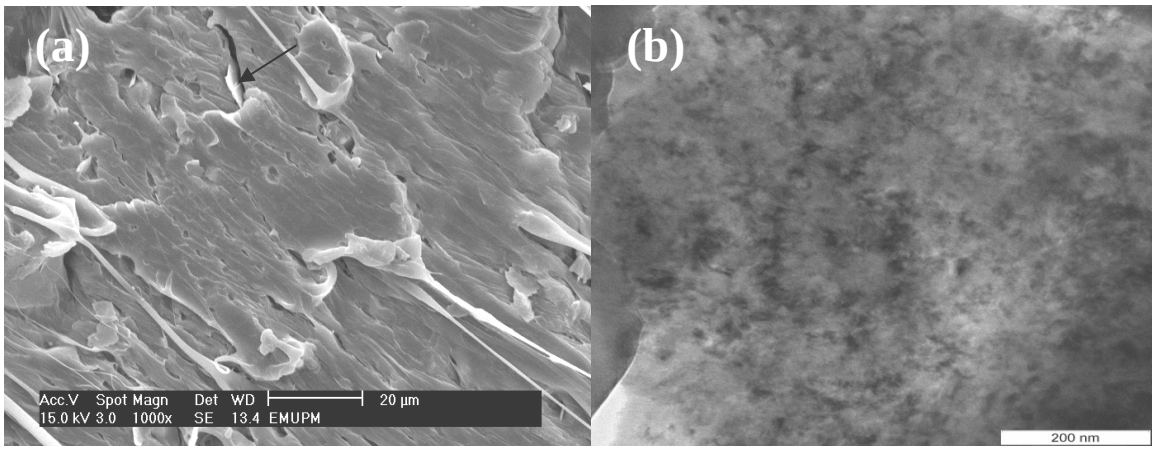

Figure 6: (a)SEM and (b) TEM micrograph of p-PLA/0.3 wt% xGnP.

ISSN 1675-7009

CONCLUSIONS

EPO plasticized and xGnP filled nanocomposites were successfully prepared by the melt blending method. The prepared nanocomposites exhibited a significant improvement in mechanical properties at a low xGnP loading. At 0.3 wt% xGnP loading, the elongation at break attained maximum values, with an increase of 3322% and 61% compared to pristine PLA and p-PLA, respectively. The enhancement to some extent of the mechanical properties of the PLA/EPO/xGnP nanocomposites can be ascribed to the homogeneous dispersion and orientation of the xGnP nanoplatelets in the polymer matrix and strong interfacial interactions between both components. Plasticized PLA reinforced with xGnP showed that increasing the xGnP content triggers a substantial increase in thermal stability. SEM results prove the enhancement of tensile strength and elongation at break at 0.3 wt% xGnP loading. The TEM micrograph of PLA/EPO/xGnP shows that the xGnP was uniformly dispersed in the PLA matrix and no obvious aggregation was observed.

REFERENCES

[1] L.V. Labrecque, R.A. Kumar, V. Davé, R.A. Gross and S.P. McCarthy, 1997. Citrate esters as plasticizers for poly(lactic acid), *Journal of Applied Polymer Science,* 66, pp. 1507-1513.

[2] N. Ljungberg, T. Andersson and B. Wesslén, 2003. Film extrusion and film weldability of poly(lactic acid) plasticized with triacetine and tributyl citrate, *Journal of Applied Polymer Science*, 88, pp. 3239-3247.

[3] M. Baiardo, G. Frisoni, M. Scandola, M. Rimelen, D. Lips, K. Ruffieux and E. Wintermantel, 2003. Thermal and mechanical properties of plasticized poly(L-lactic acid), *Journal of Applied Polymer Science,* 90, pp. 1731-1738.

[4] N. Ljungberg and B. Wesslén, 2003. Tributyl citrate oligomers as plasticizers for poly (lactic acid): thermo-mechanical film properties and aging, *Polymer*, 44, pp. 7679-7688.

[5] N. Ljungberg and B. Wesslén, 2002. The effects of plasticizers on the dynamic mechanical and thermal properties of poly(lactic acid), *Journal of Applied Polymer Science,* 86, pp. 1227-1234.

[6] O. Martin and L. Avérous, 2001. Poly(lactic acid): plasticization and properties of biodegradable multiphase systems, *Polymer*, 42, pp. 6209-6219.

[7] N. Ljungberg, D. Colombini and B. Wesslén, 2005. Plasticization of poly(lactic acid) with oligomeric malonate esteramides: Dynamic mechanical and thermal film properties, *Journal of Applied Polymer Science,* 96, pp. 992-1002.

[8] N. Ljungberg and B. Wesslén, 2005. Preparation and Properties of Plasticized Poly(lactic acid) Films, *Biomacromolecules,* 6, pp. 1789-1796.

[9] S. Jacobsen and H.G. Fritz, 1999. Plasticizing polylactide—the effect of different plasticizers on the mechanical properties, *Polymer Engineering & Science,* 39, pp. 1303-1310.

ISSN 1675-7009

[10] V.S.G. Silverajah, N.A. Ibrahim, W.M.Z.W. Yunus, H.A. Hassan and B.W. Chieng, 2012. A Comparative Study on the Mechanical, Thermal and Morphological Characterization of Poly(lactic acid)/Epoxidized Palm Oil Blend, *International Journal of Molecular Sciences,* 13, pp. 5878-5898.
[11] V.S.G. Silverajah, N.A. Ibrahim, N. Zainuddin, W.M.Z.W. Yunus and H.A. Hassan, 2012. Mechanical, Thermal and Morphological Properties of Poly(lactic acid)/Epoxidized Palm Olein Blend, *Molecules,* 17, pp. 11729-11747.
[12] N. Wang, X. Zhang, J. Yu and J. Fang, 2008. Study of the properties of plasticized poly(lactic acid) with poly(1,3-butylene adipate), *Polymers and Polymer Composites,* 16, pp. 597-604.
[13] B.W. Chieng, N.A. Ibrahim, W.M.Z. Wan Yunus and M.Z. Hussein, 2013. Plasticized poly(lactic acid) with low molecular weight poly(ethylene glycol): Mechanical, thermal, and morphology properties, *Journal of Applied Polymer Science,* 130, pp. 4576-4580.
[14] B.W. Chieng, N.A. Ibrahim, W.M.Z. Wan Yunus and M.Z. Hussein, 2014. Poly(lactic acid)/Poly(ethylene glycol) Polymer Nanocomposites: Effects of Graphene Nanoplatelets, *Polymers,* 6, pp. 93-104.
[15] E. Piorkowska, Z. Kulinski, A. Galeski and R. Masirek, 2006. Plasticization of semicrystalline poly(l-lactide) with poly(propylene glycol), *Polymer,* 47, pp. 7178-7188.
[16] Z. Kulinski, E. Piorkowska, K. Gadzinowska and M. Stasiak, 2006. Plasticization of Poly(l-lactide) with Poly(propylene glycol), *Biomacromolecules,* 7, pp. 2128-2135.
[17] Y.C. Tu, P. Kiatsimkul, G. Suppes and F.H. Hsieh, 2007. Physical properties of water-blown rigid polyurethane foams from vegetable oil-based polyols, *Journal of Applied Polymer Science,* 105, pp. 453-459.
[18] S. Gumus, G. Ozkoc and A. Aytac, 2011. Plasticized and unplasticized PLA/organoclay nanocomposites: Short- and long-term thermal properties, morphology, and nonisothermal crystallization behavior, *Journal of Applied Polymer Science,* 123, pp. 2837-2848.
[19] C.-S. Wu and H.-T. Liao, 2007. Study on the preparation and characterization of biodegradable polylactide/multi-walled carbon nanotubes nanocomposites, *Polymer,* 48, pp. 4449-4458.
[20] M.-F. Chiang and T.-M. Wu, 2010. Synthesis and characterization of biodegradable poly(l-lactide)/layered double hydroxide nanocomposites, *Composites Science and Technology,* 70, pp. 110-115.
[21] A.K. Geim, 2009. Graphene: Status and Prospects, *Science,* 324, pp. 1530-1534.
[22] K. Kalaitzidou, H. Fukushima and L.T. Drzal, 2007. Mechanical properties and morphological characterization of exfoliated graphite-polypropylene nanocomposites, *Composites Part A: Applied Science and Manufacturing,* 38, pp. 1675-1682.
[23] T. Kuila, S. Bhadra, D. Yao, N.H. Kim, S. Bose and J.H. Lee, 2010. Recent advances in graphene based polymer composites, *Progress in Polymer Science,* 35, pp. 1350-1375.
[24] V. Causin, C. Marega, A. Marigo, G. Ferrara and A. Ferraro, 2006. Morphological and structural characterization of polypropylene/conductive graphite nanocomposites, *European Polymer Journal,* 42, pp. 3153-3161.
[25] I.M. Inuwa, A. Hassan, S.A. Samsudin, M.K.M. Haafiz, M. Jawaid, K. Majeed and N.C.A. Razak, 2014. Characterization and mechanical properties of exfoliated graphite

ISSN 1675-7009

nanoplatelets reinforced polyethylene terephthalate/polypropylene composites, *Journal of Applied Polymer Science,* 131, pp. n/a-n/a.

[26] A. Yasmin, J.-J. Luo and I.M. Daniel, 2006. Processing of expanded graphite reinforced polymer nanocomposites, *Composites Science and Technology,* 66, pp. 1182-1189.

[27] X. Zhao, Q. Zhang, D. Chen and P. Lu, 2010. Enhanced Mechanical Properties of Graphene-Based Poly(vinyl alcohol) Composites, *Macromolecules,* 43, pp. 2357-2363.

[28] A. Ladhari, H. Ben Daly, H. Belhadjsalah, K.C. Cole and J. Denault, 2010. Investigation of water absorption in clay-reinforced polypropylene nanocomposites, *Polymer Degradation and Stability,* 95, pp. 429-439.

[29] Y. Xu, W. Hong, H. Bai, C. Li and G. Shi, 2009. Strong and ductile poly(vinyl alcohol)/graphene oxide composite films with a layered structure, *Carbon,* 47, pp. 3538-3543.

[30] X. Li, Y. Xiao, A. Bergeret, M. Longerey and J. Che, 2014. Preparation of polylactide/graphene composites from liquid-phase exfoliated graphite sheets, *Polymer Composites,* 35, pp. 396-403.

[31] I.-H. Kim and Y.G. Jeong, 2010. Polylactide/exfoliated graphite nanocomposites with enhanced thermal stability, mechanical modulus, and electrical conductivity, *Journal of Polymer Science Part B: Polymer Physics,* 48, pp. 850-858.

ISSN 1675-7009